Dimers of Triarylpyrylium Salts: Geometry and Electronic Transitions

Isabelle Lampre,[†] Dimitra Markovitsi,*[,†] and Philippe Millié[‡]

Laboratoire de Photophysique et de Photochimie, SCM, CNRS-URA 331, and Laboratoire de Chimie Théorique, SPAM, CEA/Saclay, DRECAM, 91191 Gif-sur-Yvette, France

Received: July 11, 1996; In Final Form: October 1, 1996[⊗]

The present paper deals with the geometry and the electronic transitions of ion-pair dimers formed by 2,6-diphenyl-4-(4′-(dialkylamino)phenyl)pyrylium tetrafluoroborates. The geometry is determined theoretically by minimizing the potential interaction energy calculated at a molecular level. The most stable configuration corresponds to a noncentrosymmetric oyster-like arrangement where the anions are sandwiched between the pyrylium cores forming an angle of *ca*. 30°. Such an arrangement is corroborated by ^{1}H-NMR and nonlinear optical measurements. The properties of the electronic transitions of the dimers are determined in the framework of the exciton theory, taking into account the calculated geometry, and compared to those obtained experimentally. It is shown that fluorescence originates from an excited state localized on one of the chromophores. Localization of the excitation is accompanied by a moving of the counterions by *ca*. 1.5 Å, due to the variation of the atomic charge distribution. The calculated decrease (3350 cm^{-1}) in the transition energy upon relaxation is practically the same as the experimentally observed Stokes shift (3000 ± 400 cm^{-1}).

1. Introduction

The interaction of light with organized molecular systems and, in particular, the electronic transitions related to photon absorption and emission, depend on both the electronic structure of the chromophores and the molecular arrangement. As a result, aggregation of dye molecules in solution is usually deduced from a change of the absorption spectra observed upon increasing concentration. The simplest molecular aggregates, dimers, have, in general, well-defined optical properties, suggesting a well-defined molecular arrangement. In spite of this fact, the geometry of dimers has not been determined experimentally so far. Although NMR measurements provide some structural information,[1−3] the precise position of the two monomers within the dimer is not known.

The geometry of several dimers was derived from their electronic absorption spectra on the basis of the exciton theory.[4−6] According to this approach, the spectral shifts observed upon dimerization are compared to those predicted by Kasha for some specific arrangements of transition moments.[7] A spectral analysis yields the coupling between the transition moments of the two monomers and the oscillator strength of the two dimer transitions. Then, using either the point dipole or the extended dipole approximation, the relative orientation and the distance between the monomers are deduced. However, as pointed out in ref 8, the location of the dipole within the molecules is problematic, especially for asymmetric dyes. Consequently, the resulting arrangement depends on this positioning. Anyway, the geometry of dimers is governed by intermolecular forces and may be quite complex.

We reported previously that the 2,6-diphenyl-4-(4′-(dialkylamino)phenyl)pyrylium salts {P_{1-12^+}, BF_4^-} and {P_{12-12^+}, BF_4^-} shown in Figure 1 form ion-pair dimers in nonpolar solvents.[9,10] A nontrivial geometrical structure was invoked to interpret their quite unusual optical properties. Indeed, these ion-pair dimers are capable of generating second harmonic in solution.[11] It was also found that the transition moment corresponding to fluorescence is orthogonal to the moment of the lowest in energy transition associated with absorption. Moreover, the fluorescence maximum is shifted by *ca*. 3000 cm^{-1} with respect to the maximum of the lowest in energy absorption band. The drastic change in the wave function of the lowest excited state is not hindered in solid matrices, proving that the dimer geometry possesses certain degrees of freedom, even in a rigid environment. The relaxation process was interpreted in terms of counterion motion caused by the photoinduced change of the atomic charge distribution of the triarylpyrylium chromophores.

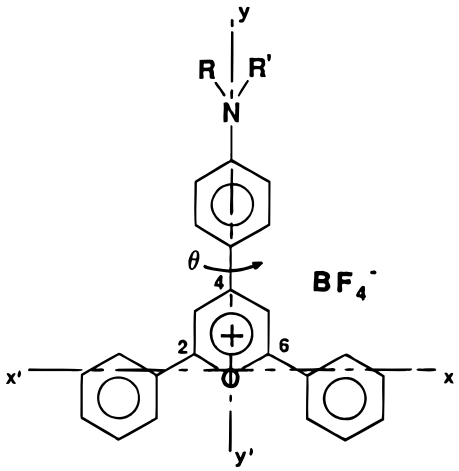

Figure 1. Schematic representation of the studied 2,6-diphenyl-4-(4′-(dialkylamino)phenyl)pyrylium tetrafluoroborates: P_{1-1^+}, R = R′ = CH_3; P_{1-12^+}, R = CH_3, R′ = $C_{12}H_{25}$; P_{12-12^+}, R = R′ = $C_{12}H_{25}$. θ denotes the dihedral angle formed between the pyrylium core and the plane of the aryl group.

As a continuation of our previous experimental study,[9−12] the aim of the present work is to correlate the properties of the electronic transitions of the triarylpyrylium dimers to both the molecular arrangement and the electronic structure of the ionic components (two cations and two anions). For this purpose, we have undertaken a theoretical investigation based on quantum chemistry methods and the exciton theory.

[†] Laboratoire de Photophysique et de Photochimie.
[‡] Laboratoire de Chimie Théorique.
[⊗] Abstract published in *Advance ACS Abstracts,* December 1, 1996.

S1089-5639(96)02066-X CCC: $14.00

In section 2, we present the dimer geometry determined by minimizing the potential interaction energy expressed as the sum of electrostatic, polarization, dispersion, and repulsion terms. This methodology, initially developed to find out the conformation of biological systems,[13,14] was recently applied in the case of van der Waals complexes formed in the gas phase.[15,16] In order to explore the whole potential energy surface of the examined triarylpyrylium dimers, a simulated annealing method[17] is used.

In section 3, we tackle the properties of the transitions related to absorption in the visible spectral domain, hereafter referred to as "Franck−Condon" transitions. We calculate their moment within the geometry determined in section 2 and using the coupling values deduced from the experimental absorption spectra. Then, we discuss the relaxation process. We quantify the counterion motion associated with the change of the atomic charge distribution of the triarylpyrylium chromophores upon excitation. Moreover, we evaluate the change in the energy and polarization of the lowest singlet transition associated with this motion.

2. Ground State Geometry

A comparative spectroscopic study of the triarylpyrylium cations P_{1-1}^+, P_{1-12}^+, and P_{12-12}^+, revealed that addition of one or two dodecyl chains on the nitrogen atom has practically no influence on the electronic transitions of the triarylpyrylium chromophores.[9,10,12] The properties (equilibrium constant, absorption and fluorescence spectra, fluorescence lifetimes, and quantum yields) of the dimers formed in nonpolar solvents by $(P_{12-12}^+, BF_4^-)_2$ are practically the same as those of $(P_{1-12}^+, BF_4^-)_2$.[10] Hence, calculations are performed for $(P_{1-1}^+, BF_4^-)_2$ dimers, although these species are not experimentally observed because the $\{P_{1-1}^+, BF_4^-\}$ salt is not soluble in nonpolar solvents. Moreover, the photophysical properties of the examined dimers are not affected by the molecular structure, polarizability, and dielectric constant of the solvent; *i.e.* they are similar in chloroform, toluene,[10] dioxane, or ether.[18] For this reason, the influence of the solvent is neglected.

2.1. General Procedure. The geometry of an aggregate is defined by $6(M - 1)$ degrees of freedom, corresponding to the Euler angles and the positional coordinates of the M constitutive chemical species. For the $(P_{1-1}^+, BF_4^-)_2$ dimer, composed of two cations and two anions, M equals four. Its potential energy as a function of the 18 degrees of freedom is represented by a 18-dimensional potential energy surface. In order to determine the minima of this surface, a simulated annealing method[17] was used. For each temperature step, a random search was performed by the Metropolis algorithm, and the most stable configurations obtained from this exploration were sorted out. After having repeated the annealing four times, 400 configurations were optimized by a local minimization method (quasi Newton method, BFGS[19]), providing a series of local minima.

This procedure is based on the intermolecular interaction energy derived from the net charge and elementary dipoles located on each atom of the considered ions. It is assumed that the charge distribution is that of the "isolated" ions; that is, no charge transfer occurs between the anion and the cation. This hypothesis has been checked by the study of the ion pair (the charged chromophore and its counterion) as a "supermolecule".[18]

2.2. Calculation Details. The atomic charge distribution of the examined ions was determined by the CS INDO method.[20] The INDO parameters (screening factors for the resonance integrals, one-center and two-center integrals) were taken from ref 21. The structural parameters of P_{1-1}^+ used were those reported in ref 12. The dihedral angle θ (Figure 1), formed between the pyrylium core and the aryl group at position 4, was considered as an adjustable parameter because its value greatly depends both on the aryl groups and the local environment.[12,25] A T_d tetrahedral symmetry was considered for BF_4^-, and the B−F bond length was taken to be equal to 1.365 Å.[22]

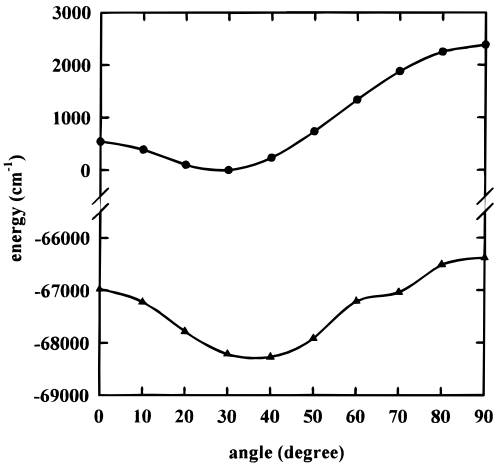

Figure 2. Energy of two P_{1-1}^+ free cations (●) and the $(P_{1-1}^+, BF_4^-)_2$ dimer (▲) as a function of the dihedral angle θ (cf. Figure 1); for each angle θ the positions of the two anions and the two cations are optimized.

The polarizabilities used for the calculation of the polarization term were deduced from experimental data.[23] However, no experimental value was available for the B−F bond. An estimation ($\alpha = 0.623$ Å^3) was obtained at the SCF level, by means of the HONDO program.[24]

The initial temperature of the annealing method was chosen equal to 2000 K assuming that the corresponding thermal energy (kT) was higher than the energy barriers. Moreover, an upper limit for the interaction energy (-3500 cm^{-1}) and a maximum distance between the centers of gravity along each direction (18 Å) were imposed. These conditions were utilized to limit the exploration of the potential energy surface to the area corresponding to dimer formation.

2.3. Results and Discussion. The energy of the dimer is defined by the energy of two free cations and the energy of two free anions plus the total potential interaction energy. First, we consider dimers in which the angle θ is the same for the two cations. Figure 2 shows the energy of two P_{1-1}^+ free cations and that of the $(P_{1-1}^+, BF_4^-)_2$ dimer as a function of θ. For each angle θ, the positions of the two anions and the two cations were optimized and the absolute minimum obtained for the energy is reported. The energy of the two anions does not depend on θ, and it is taken to be equal to zero. We remark in Figure 2 that the dimer energy is minimum when θ ranges from 30 to 40°. The rotational energy barriers corresponding to $\theta =$ 0 and 90° are 1240 and 1835 cm^{-1}, respectively. These values show that simultaneous rotation of the two (dimethylamino)-phenyl groups is hindered at room temperature ($kT = 200$ cm^{-1}). Moreover, for each angle θ, the energy difference between the absolute minimum and the other local minima is bigger than the Boltzmann factor at room temperature. The only exception appears at $\theta = 60°$ where two isoenergetic configurations exist. Upon increasing or decreasing θ from 60°, one or the other of these two configurations is favored. This results in an inflection point on the dimer curve (Figure 2).

Considering the minimum area of the dimer energy curve (Figure 2), we have estimated the effect produced when the two cations are not strictly identical. For this purpose, we have fixed the angle θ of one chromophore ($\theta = 30$ or 40°) and varied the angle θ of the other. The minimum energy is found when the angles of both chromophores range from 30 to 40°. Moreover, we performed an annealing process taking $\theta = 30°$ for one

triarylpyrylium cation and $\theta = -30°$ for the other (each cation is the mirror image of the other). The minimum interaction energy obtained from this exploration is higher than that corresponding to two identical cations ($\theta = 30°$). It is worth remembering that the dihedral angle θ determined by the INDO method for the most stable configuration of the free P_{1-1}^+ cation is 30°.[12] Consequently, θ is practically unaffected by dimerization.

In order to unravel the nature of the forces responsible for the dimerization of triarylpyrylium tetrafluoroborates, we calculated the enthalpy ΔH of the dimer formation corresponding to the equilibrium

$$2(P_{1-1}^+, BF_4^-) \rightleftarrows (P_{1-1}^+, BF_4^-)_2$$

as the difference between the stabilization energy of the dimer, $(P_{1-1}^+, BF_4^-)_2$, and that of two ions pairs, (P_{1-1}^+, BF_4^-). We found that for any value of θ, the stabilization energy of the dimer is higher than twice the stabilization energy of the ion pair, proving that the dimer is always more stable than two ion pairs. Using the values determined for the most stable configuration ($\theta = 30°$) of the dimer and the ion pair, ΔH is found to be -9500 cm^{-1}. This value is the sum of electrostatic, polarization, dispersion, and repulsion terms whose contributions are respectively -3900, -2800, -5300, and 2500 cm^{-1}. We remark that the predominant interaction leading to the dimer stabilization is the dispersion one. However, the overall electrostatic interaction is negative although it contains positive repulsive terms, showing that the proximity of two ion pairs are electrostatically favored. In contrast, when we consider only two triarylpyrylium cations, the overall electrostatic interaction is always positive and is not compensated by the polarization and dispersion terms. This proves that the counterions are indispensable to aggregation.

Figure 3 shows two different views of the most stable geometry of the $(P_{1-1}^+, BF_4^-)_2$ dimer. This geometry, hereafter referred to as geometry G, differs from a typical parallel head-to-tail arrangement commonly assumed for dimers. The planes determined by the two phenyl groups and the pyrylium core of each chromophore form a dihedral angle of *ca.* 30°. If the dimer is viewed along the *zz′* axis of one chromophore, one can see that the *yy′* axes of the two cations form an angle of *ca.* 160°. The two counterions are sandwiched between the two pyrylium planes, resulting in an oyster-like geometry. It should be emphasized that, despite the noncentrosymmetric molecular arrangement, the two cations chromophores (respectively the two anions) are equivalent in the dimer. As a matter of fact, they have the same polarization energy, and the interaction energy between one of the cations and one of the anions is identical to the interaction energy between the other cation and the other anion.

We also determined the geometry of the dimers corresponding to the other local minima of the simulated annealing. All the most stable configurations whose interaction energy is located within a range of 1000 cm^{-1} (from $-68\,200$ to $-67\,200$ cm^{-1}) are quite similar to that shown in Figure 3: the cations are not parallel, and the two anions are sandwiched between them.

2.4. Comparison with Experimental Results. As a first step, it is interesting to evaluate the enthalpy and the entropy related to dimer formation and compare them to the corresponding values reported in the literature. The entropy ΔS can be estimated from the equations

$$\Delta G = \Delta H - T\Delta S \quad (1)$$

$$\Delta G = -RT \ln K \quad (2)$$

where ΔG, ΔH, K, R, and T are the free energy, the enthalpy, the dimerization constant, the gas constant, and the temperature, respectively. Using the dimerization constant determined for $(P_{1-12}^+, BF_4^-)_2$ in toluene at 300 K (2.7×10^5 dm^3 mol^{-1}) and the enthalpy ΔH calculated in section 2.3 (-27 kcal mol^{-1}), ΔS is found to be equal to -67 cal mol^{-1} K^{-1}. The latter value is negative, in agreement with a decrease in the number of independently moving species and an increase of the order of the system. Moreover, both the entropy ΔS and the enthalpy ΔH values are of the same order of magnitude as those experimentally found for dimerization of rhodamine dyes.[6,26−28]

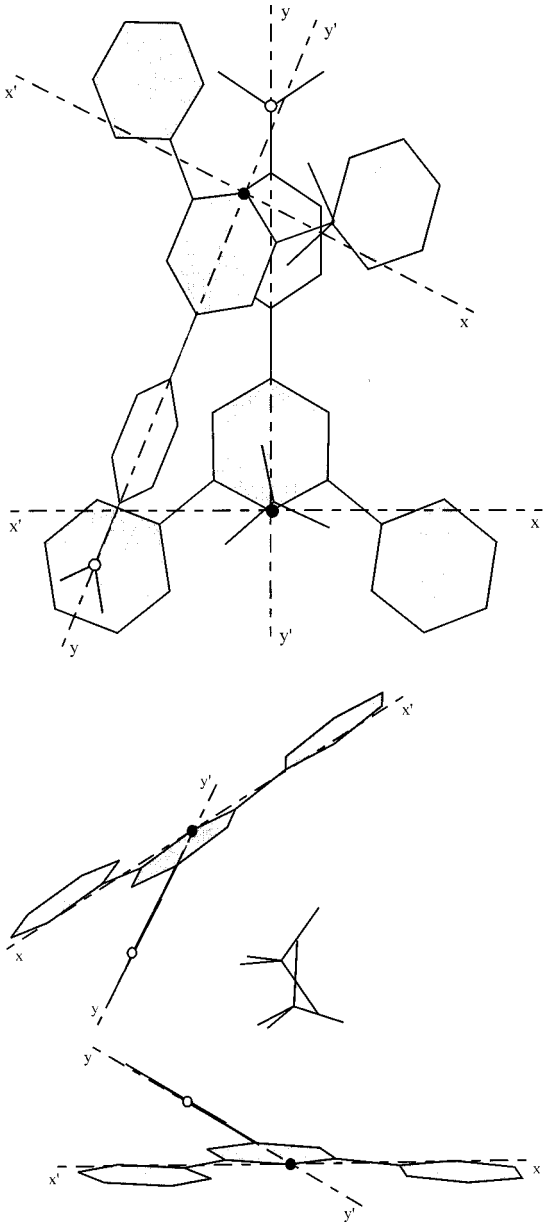

Figure 3. Two different views of the most stable geometry G of the $(P_{1-1}^+, BF_4^-)_2$ dimer. In grey are shown the two phenyl groups and the pyrylium core of each chromophore lying in the same plane. The oxygen and nitrogen atoms are represented as black and white disks, respectively.

The oyster-like geometry determined by our calculations, in which the small anions are sandwiched between the large cations, is in agreement with the experimental finding[9] that only dimers and not higher order aggregates are formed in solution. Indeed, if the dimer structure was characterized by either a stacking of planar ion pairs or an alternative stacking of anions and cations, no limitation of the aggregation number would be expected. Moreover, the noncentrosymmetric arrangement is corroborated by the fact that the dimers are capable of generating second harmonic.

TABLE 1: Properties[a] of the Dimer Electronic Transitions Determined Experimentally[11]

		$\|0\rangle \rightarrow \|1\rangle$	$\|0\rangle \rightarrow \|2\rangle$	$\|0\rangle \rightarrow \|3\rangle$	$\|0\rangle \rightarrow \|4\rangle$
$(P_{1-1}^{+}, BF_4^{-})_2$ in polystyrene	E (cm^{-1})	16 500	17 950	19 290	20 700
	$\|\|\mu_{ex}\|\|$(D)	2.5	6.6	10.1	4.8
	r ($\pm$0.02)	−0.20	0.13	0.30	0.11
$(P_{1-1}^{+}, BF_4^{-})_2$ in toluene	E (cm^{-1})	16 800	18 400	19 650	20 900
	$\|\|\mu_{ex}\|\|$(D)	2.1	5.2	10.7	4.9
$(P_{12-12}^{+}, BF_4^{-})_2$ in toluene	E (cm^{-1})	16 500	18 050	19 350	20 600
	$\|\|\mu_{ex}\|\|$(D)	2.0	5.4	9.9	4.7

[a] E = energy, $||\mu_{ex}||$ = transition moment, and r = fluorescence excitation anisotropy.

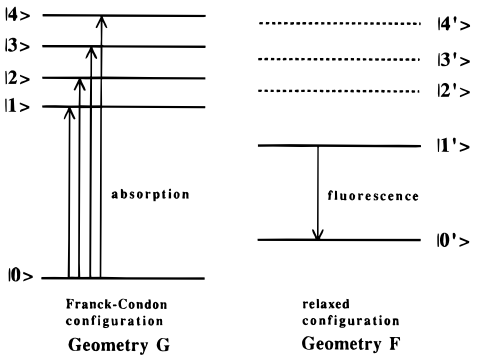

Figure 4. Simplified diagram of the dimer excited states in the Franck−Condon geometry G and in the geometry F reached after relaxation.

Finally, the most stable geometry determined for $(P_{1-1}^{+}, BF_4^{-})_2$ has to be compared to the structural data obtained for $(P_{12-12}^{+}, BF_4^{-})_2$ by two-dimensional ^{1}H-NMR ROESY experiments.[10] The maximum stabilization energy of the dimer is observed for configurations having a dihedral angle θ ranging from 30 to 40° (Figure 2). This value is in very good agreement with the value deduced from ^{1}H-NMR experiments (32°). Moreover, these experiments have revealed that there is at least one pair of protons formed by one proton **a** of the one cation and one proton **d** of the other (see Figure 5 in ref 10), located at a distance shorter than 5 Å. The same statement is also valid for the pairs formed by one proton **α** of the one cation and one proton **d** of the other. The shortest distances calculated for the geometry G shown in Figure 3 are 3.2 and 3.8 Å for the pairs (**a**, **d**) and (**α**, **d**), respectively. We remark that distances shorter than 5 Å are possible only if the pyrylium cores, separated by the counterions, are not parallel.

3. Electronic Transitions

In this part of our investigation, we examine if the calculated oyster-like geometry may explain the photophysical properties determined experimentally.[9−11] Our approach is based on the exciton theory according to which the dimer excited states are delocalized on both cationic chromophores and are linear combinations of the excited states localized on each monomeric unit. We use the neutral exciton model neglecting all the intermolecular charge transfer states. This is understandable for two reasons. First, we found no charge transfer between P_{1-1}^{+} and BF_4^{-} by calculating the first two excited states of the ion pair (P_{1-1}^{+}, BF_4^{-}) as a "supermolecule". Second, a charge transfer between the two cationic chromophores (P_{1-1}^{++}, P_{1-1}) is not probable since, in the considered geometry, the orbital overlap between the two triarylpyrylium cations is very weak, the mean interchromophore distance being *ca*. 5 Å.

The properties of the electronic transitions obtained from spectral analysis[11] are summarized in Table 1 and illustrated in the simplified diagram of Figure 4. We recall that the absorption of the dimer in the visible spectral domain corresponds to four electronic transitions, associated with the two transitions of each triarylpyrylium cation (2 × 2). The energy and polarization of the transition corresponding to fluorescence are quite different from those of the lowest Franck−Condon transition.

Before discussing in detail the electronic transitions, both in the Franck−Condon configuration (section 3.2) and after relaxation (section 3.3), we present the general formalism of the exciton theory adapted in the particular case of the studied system (section 3.1). More precisely, we take into account the existence of two electronic transitions ($S_0 \rightarrow S_y$ and $S_0 \rightarrow S_x$) close in energy and polarized along the yy' and xx' axes of each chromophore (Figure 1). This approach, already developed in the case of columnar aggregates formed by triarylpyrylium salts,[29] is necessary when the energy difference between the two localized states is of the same order of magnitude as the coupling between transition moments.

3.1. General Formalism. The total electronic Hamiltonian **H** of the system is

$$\mathbf{H} = \mathbf{H}_1 + \mathbf{H}_2 + \mathbf{H}_{int} \tag{3}$$

$\mathbf{H}_1$, $\mathbf{H}_2$, and $\mathbf{H}_{int}$ denote respectively the Hamiltonian of the two chromophores and the Hamiltonian describing the interactions among the various components of the aggregate. We use as a basis set for the ground state and the 2 × 2 excited states of the system the eigenrepresentations of $\mathbf{H}_1 + \mathbf{H}_2$, namely

$$\Psi^0 = |\phi_1^0 \phi_2^0\rangle \tag{4}$$

$$\Psi_1^i = |\phi_1^i \phi_2^0\rangle \tag{5}$$

$$\Psi_2^i = |\phi_1^0 \phi_2^i\rangle \tag{6}$$

ϕ_n^0 and ϕ_n^i denote respectively the wave functions of the ground state and the singlet excited state S_i ($i = x, y$) of the isolated chromophore n ($n = 1, 2$). The total Hamiltonian matrix is written as follows

$$\mathbf{H} = \begin{bmatrix} E_1^y & 0 & V_{yy} & V_{yx} \\ 0 & E_1^x & V_{xy} & V_{xx} \\ V_{yy} & V_{xy} & E_2^y & 0 \\ V_{yx} & V_{xx} & 0 & E_2^x \end{bmatrix} \tag{7}$$

where E_n^i is the energy of the S_i state of the chromophore n within the dimer, while V_{ij} designates the coupling between the $S_0 \rightarrow S_i$ transition of the first chromophore and the $S_0 \rightarrow S_j$ transition of the second chromophore. The terms equal to 0 correspond to the coupling between transitions of the same chromophore which are orthogonal.

A full diagonalization of the Hamiltonian provides the four eigenstates, $|1\rangle$, $|2\rangle$, $|3\rangle$, and $|4\rangle$, of the dimer and their energies E_k (k = 1, 2, 3, and 4)

$$|k\rangle = C_{y,1}^k \Psi_1^y + C_{x,1}^k \Psi_1^x + C_{y,2}^k \Psi_2^y + C_{x,2}^k \Psi_2^x \tag{8}$$

with the normalization condition

$$\sum_{i,n} C_{i,n}^{k} C_{i,n}^{l} = \delta_{k,l} \tag{9}$$

The coefficients $C_{i,n}^{k}$ of the linear combination (eq 8) represent the contribution of the excited state S_i of the chromophore n to the eigenstate $|k\rangle$ of the dimer. The transition moment $\boldsymbol{\mu}^k$ associated with a given collective state is

$$\boldsymbol{\mu}^k = C_{y,1}^{k}\boldsymbol{\mu}_1^{y} + C_{x,1}^{k}\boldsymbol{\mu}_1^{x} + C_{y,2}^{k}\boldsymbol{\mu}_2^{y} + C_{x,2}^{k}\boldsymbol{\mu}_2^{x} \tag{10}$$

μ_n^i denotes the $S_0 \rightarrow S_i$ transition of the chromophore n. It should be stressed that in eq 10 all the transition moments are vectors.

3.2. Franck−Condon Transitions. The main question to be answered is whether a set of linear combinations of the monomer transition moments $\boldsymbol{\mu}^x$ and $\boldsymbol{\mu}^y$ may yield, within the examined geometry G, the transition moments of the dimer shown in Table 1. In particular, it is to be wondered if the third transition $|0\rangle \rightarrow |3\rangle$ may be the strongest one. As a matter of fact, the transition moments of the dimer eigenstates depend on both the geometry and the terms of the Hamiltonian matrix **H**. The geometry plays a key role in the vectorial sum given by eq 10.

The ground state energy of the dimer taken as zero, and the energies of the dimer electronic transitions listed in Table 1 correspond to the eigenvalues E_k of **H**. This means that the result of diagonalization of the Hamiltonian matrix is known. Consequently, under certain conditions, it is possible to determine the diagonal and off-diagonal terms of the matrix and then deduce the coefficients of the linear combinations $C_{i,n}^{k}$. As the two triarylpyrylium chromophores are equivalent within the geometry G, we have $E_1^y = E_2^y = E_y$, $E_1^x = E_2^x = E_x$, and $V_{xy} = V_{yx}$. Moreover, due to the quasi antiparallel arrangement of the yy' axes of the two triarylpyrylium cations, the sign of V_{yy} must be opposite to that of V_{xx}. E_y and E_x are the excitation energies of the localized transitions within the local environment of the dimer and may be slightly different from the corresponding values determined for the monomer (17 900 and 19 300 cm^{-1}, respectively[11] in chloroform). Therefore, we considered a series of E_x values located in the visible spectral area of interest and distant of 100 cm^{-1}. For each one of these E_x values, E_y, V_{yy}, V_{xy}, and V_{xx} were determined by resolving a system of four equations with four unknowns. The procedure followed for the resolution of the system is described in detail in the Appendix.

Figure 5 shows the values of the diagonal and off-diagonal terms of the Hamiltonian matrices having as eigenvalues the energies of the dimer excited states found experimentally for $(P_{1-12}^{+}, BF_4^{-})_2$ in toluene (Table 1). The system of four equations with four unknowns can be resolved only when E_x ranges either from 17 600 to 18 300 cm^{-1} or from 19 600 to 20 300 cm^{-1}. These two energy domains correspond to mathematically equivalent solutions of the system. From a physical point of view, in the former domain, the order of the localized states is inversed with respect to that in the latter. Such an inversion, caused by the local environment, was theoretically demonstrated for columnar aggregates formed by discotic triarylpyrylium derivatives.[29]

We remark that $|V_{yy}|$ and $|V_{xx}|$ are of the same order of magnitude (1000 ± 400 cm^{-1}) and close to the values reported in the literature for dimers. The difference between them is quite small and practically independent of the E_x value (*ca*. 175 cm^{-1}). Moreover, all the $|V_{xy}|$ values are located above 300 cm^{-1}, and consequently, they are higher than the Boltzmann factor at room temperature (200 cm^{-1}). Surprisingly, upon splitting apart the states S_y and S_x, $|V_{xy}|$ increases, reaches a maximum, and then diminishes again.

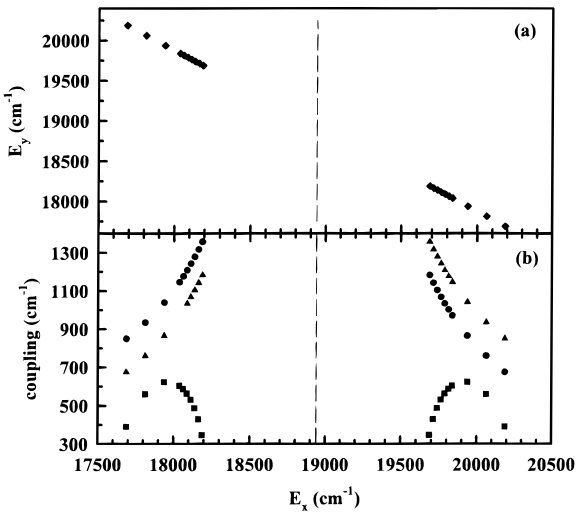

Figure 5. Diagonal (a) and off-diagonal (b) terms of the Hamiltonian matrices having as eigenvalues the energies of the dimer transitions found for $(P_{1-12}^{+}, BF_4^{-})_2$ in toluene (Table 1). The absolute values of the off-diagonal terms V_{yy} (▲), V_{xx} (●), and V_{xy} (■) are represented. The dashed line indicates the value corresponding to $E_x = E_y$.

TABLE 2: Coordinates of the Localized Transition Moments (D) within the Geometry G of the Dimer[a]

	μ_1^y	μ_1^x	μ_2^y	μ_2^x
μ_x	0.0	−5.1	3.2	−3.7
μ_y	−8.4	0.0	7.7	1.9
μ_z	0.0	0.0	1.0	−2.9

[a] $\boldsymbol{\mu}_n^i$ denotes the $S_0 \rightarrow S_i$ transition of the chromophore n. The xx', yy', and zz' axes refer to the first chromophore. The transition moments $||\boldsymbol{\mu}||$ are deduced from the experimental absorption spectra,[11] while the orientation of the vectors within the molecular frame are determined quantum mechanically.[12]

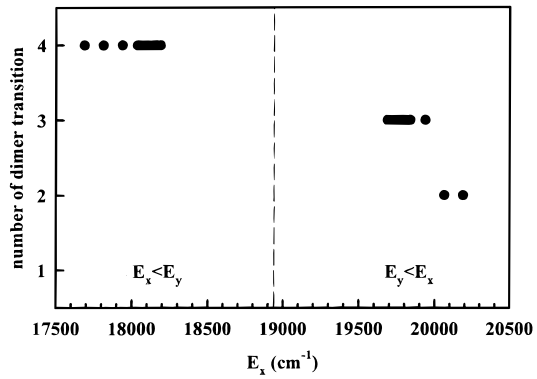

Figure 6. Number of the dimer transition having the largest transition moment, as a function of the excitation energy E_x. The transition moments are calculated taking into account the dimer geometry G and the Hamiltonian matrix corresponding to E_x (Figure 5).

For each Hamiltonian **H** defined by one of the sets of values shown in Figure 5, we determined the eigenstates, *i.e*., the coefficients of the linear combinations (eq 8). Then, taking into account the coordinates of the transition moments for each chromophore within the dimer geometry G (Table 2), we calculated the four transition moments of the dimer (eq 10). Figure 6 shows the number of dimer transition characterized by the largest moment. Upon increasing E_x, the largest moment is associated successively with $|0\rangle \rightarrow |4\rangle$, $|0\rangle \rightarrow |3\rangle$, and $|0\rangle \rightarrow |2\rangle$. Therefore, it does exist an energy domain in agreement with the experimental data according to which the maximum oscillator strength is born by the $|0\rangle \rightarrow |3\rangle$ transition (Table 1). This relatively narrow energy domain (E_x ranging from 19 600 to 19 950 cm^{-1}) belongs to the region for which E_x is higher than E_y, proving that the order of the localized states is not

TABLE 3: Franck−Condon Transition Moments (D) of the Dimer[a]

	$\|0\rangle \rightarrow \|1\rangle$	$\|0\rangle \rightarrow \|2\rangle$	$\|0\rangle \rightarrow \|3\rangle$	$\|0\rangle \rightarrow \|4\rangle$
μ_x	1.35	−0.37	2.41	−6.48
μ_y	−0.3	−4.9	10.37	1.43
μ_z	0.45	−2.13	−0.47	−2.14
$\|\|\boldsymbol{\mu}\|\|$	1.46	5.36	10.66	6.98
$\|\|\boldsymbol{\mu}_{ex}\|\|$	2.1	5.2	10.7	4.9

[a] The xx', yy', and zz' axes refer to the first chromophore. μ_x, μ_y, μ_z, $\|\|\boldsymbol{\mu}\|\|$ = coordinates and length of the vectors calculated (eq 10) by taking into account the geometry G and the eigenvectors corresponding to **H** defined by $E_y = 18\,090$ cm^{-1}, $E_x = 19\,790$ cm^{-1}, $V_{yy} = -1210$ cm^{-1}, $V_{xy} = -560$ cm^{-1}, and $V_{xx} = 1035$ cm^{-1}; $\|\|\boldsymbol{\mu}_{ex}\|\|$ = experimental values obtained for (P_{1-12}^+, BF_4^-)$_2$ in toluene (Table 1).[11]

TABLE 4: Components of the Dimer Eigenstates in the Basis of the Localized Excited States (Eq 8)[a]

	$C^k_{y,1}$	$C^k_{x,1}$	$C^k_{y,2}$	$C^k_{x,2}$
$\|1\rangle$	0.700	0.098	0.700	0.098
$\|2\rangle$	0.376	−0.599	−0.376	0.599
$\|3\rangle$	−0.599	−0.376	0.599	0.376
$\|4\rangle$	−0.098	0.700	−0.098	0.700

[a] The coefficients $C^k_{i,n}$ of each state $|k\rangle$ correspond to **H** defined by $E_y = 18\,090$ cm^{-1}, $E_x = 19\,790$ cm^{-1}, $V_{yy} = -1210$ cm^{-1}, $V_{xy} = -560$ cm^{-1}, and $V_{xx} = 1035$ cm^{-1}.

modified upon dimerization. Among the sets of four transition moments obtained for each E_x value, Table 3 shows the one closest to the experimental transition moments. The agreement between the calculated and experimental values is quite good, the largest difference (40%) corresponding to the $|0\rangle \rightarrow |4\rangle$ transition.[30] The diagonal terms of the Hamiltonian **H** yielding the best fit between the experimental and calculated dimer transition moments (Table 3) are 18 090 and 19 790 cm^{-1}. E_y and E_x differ respectively by 200 and 500 cm^{-1} from the energy of the $S_0 \rightarrow S_y$ and $S_0 \rightarrow S_x$ transitions, determined for the monomeric chromophore in chloroform.[11] Changes of a few hundred inverse centimeters in the excitation energy of localized transitions are also reported in the case of dimerization of rhodamine dyes.[31,32]

The components of the dimer eigenstates in the basis of the localized excited states (eq 8) corresponding to the set of calculated transition moments in Table 3 are shown in Table 4. First, we remark that, as expected, all the dimer eigenstates are symmetrically built on the two chromophores, since the two triarylpyrylium cations are equivalent within the dimer. Moreover, we notice that the lower eigenstate is almost utterly built on the two S_y localized states (98%). Likewise, the upper eigenstate is mainly built on S_x, whereas both localized states S_x and S_y contribute to the eigenstates $|2\rangle$ and $|3\rangle$ (28 and 72%).

The properties of the Franck−Condon transitions described above were obtained using as eigenvalues of the Hamiltonian **H** the transition energies found for (P_{1-12}^+, BF_4^-)$_2$ in toluene. Quite similar results are obtained if we consider the transition energies of (P_{12-12}^+, BF_4^-)$_2$ in toluene or those of (P_{1-12}^+, BF_4^-)$_2$ in polystyrene. We also evaluated the error made in the determination of the diagonal and off-diagonal terms of **H**, arising mainly from the E_k values known with a precision of ±250 cm^{-1}. A change in E_k within ±250 cm^{-1} yields different values for V_{yy}, V_{xx}, and V_{xy}, but the order of magnitude of each coupling value remains the same.

Remarks. We calculated quantum mechanically, within the INDO formalism, the interaction between the transition moments of the two triarylpyrylium cations within the geometry G. We used a methodology based on bicentric bielectronic integrals, described in detail in ref 33. We found that V_{yy}, V_{xx}, and V_{xy} are −720, 110, and −400 cm^{-1}, respectively. We remark that the calculated V_{yy} and V_{xy} values are not so different from those shown in Figure 5, but that V_{xx} is weaker by 1 order of magnitude. Such a weak calculated V_{xx} value is not so surprising, since (i) the moment of the $S_0 \rightarrow S_x$ transition is smaller than that of the $S_0 \rightarrow S_y$ one[11,12] and (ii) the phenyl groups involved in the $S_0 \rightarrow S_x$ transition of the one chromophore lie far apart from the corresponding groups of the other (Figure 3). The geometries yielding V_{xx} values as high as the V_{yy} ones are those where one cation is displaced along the zz' axis with respect to the other (head-to-head configurations). However, such molecular arrangements are counter to the results obtained by ^{1}H-NMR measurements and, also, to a high V_{xy} coupling. We do not know the origin of the discrepancy between the coupling values calculated in the framework of the INDO formalism and the values deduced from the absorption spectra. However, we are tempted to relate it to the presence of the two counterions which are sandwiched between the two chromophores and are not taken into account in the INDO calculation of the coupling.

3.3. Relaxation. The starting point of our investigation of the relaxation resides on the observation that the transition related to fluorescence is orthogonal to the lowest Franck−Condon transition. This drastic change occurs even in solid matrices where molecular rotation, although not completely inhibited (*cf.* below), is seriously hindered and where solvent relaxation is impaired. We have shown in section 3.2 that the lowest Franck−Condon state of the studied dimers is symmetrically built mainly on the localized S_y states of the two chromophores (Table 4) although the $|0\rangle \rightarrow |1\rangle$ transition is polarized essentially along the xx' axes (Table 3). As far as the lowest excited state remains symmetric, and consequently delocalized, no change in the polarization of the corresponding transition can happen because the signs of the coefficients $C^k_{i,n}$ (eq 8) will remain the same. On the contrary, localization of the excitation on one of the two chromophores induces a breakdown of the symmetry and leads to a change of polarization. Such a localization will result in the formation of a S_y state because S_y is the major component of $|1\rangle$.

Following the above conclusion, we determined the geometry F obtained from the geometry G upon relaxation, when one of the chromophores is in its S_y excited state, while the other remains in its ground state. For this purpose, we fixed the coordinates of the two triarylpyrylium cations, and we performed a local minimization of the potential interaction energy of the system as in section 2. The atomic charge distribution of S_y was obtained by configuration interaction involving only the singly excited configurations.[12] We found that relaxation involves a moving of the one counterion by 1.7 and 1.3 Å of the other, mainly along the yy' axis of the excited chromophore. This is understandable, since S_y is a charge transfer state[12] and electrostatic interactions play an important role in the positioning of counterions.

Relaxation from the delocalized state $|1\rangle$ in the geometry G toward the localized state S_y in the geometry F can take place if the energy of the stabilized S_y is lower than the energy of $|1\rangle$. The energy of S_y within the geometries G and F of the dimer is given by eqs 11 and 12, respectively

$$E_G(S_y) = E_0(S_y) + E_{inter(G)} + E_{solv(G)} \quad (11)$$

$$E_F(S_y) = E_0(S_y) + E_{inter(F)} + E_{solv(F)} \quad (12)$$

where $E_0(S_y)$ is the energy of S_y in the vacuum, E_{inter} is the potential interaction energy of the dimer within the considered geometry when one of the cations is in the excited state S_y, and E_{solv} is the interaction energy with the solvent. Taking into account that the solvent rearrangement is hindered in solid matrices and that the atomic charge distribution of the two

TABLE 5: Angles α_k (deg) Formed between the Dipole Moments Corresponding to the $|0\rangle \leftarrow |1'\rangle$ and $|0\rangle \rightarrow |k\rangle$ Transitions

	α_1	α_2	α_3	α_4
calculated[a]	78	24	13	78
experimental[b]	90	42	24	44

[a] The calculated values correspond to the angles α_k formed between the dipole moment of one $S_0 \rightarrow S_y$ transition (Table 2) and each one of the Franck−Condon transition moments $\boldsymbol{\mu}^k$ (geometry G, Table 3).[b] The experimental values are deduced from the anisotropy r_k associated with each dimer transition (Table 1) through the equation $r_k = (3 \cos^2 \alpha_k - 1)/5$.

cations, in contact with the solvent, is identical in G and in F, we set $E_{\text{solv(G)}} = E_{\text{solv(F)}}$. Thus, $E_F(S_y)$ can be expressed as a function of $E_G(S_y)$

$$E_F(S_y) = E_G(S_y) + E_{\text{inter(F)}} - E_{\text{inter(G)}} \qquad (13)$$

$E_G(S_y)$ is equal to the diagonal term of the Hamiltonian **H** of the system in the geometry G (E_y = 18 090 cm^{-1}, Table 3). The difference in the calculated interaction energies, $E_{\text{inter(F)}} - E_{\text{inter(G)}}$, is 1660 cm^{-1}. Thus, the energy $E_F(S_y)$ is found to be 16 430 cm^{-1}, which is lower than the energy of the eigenstate $|1\rangle$ (16 800 cm^{-1}). $E_F(S_y)$ corresponds to the diagonal term (E_1^y) of the Hamiltonian matrix of the system (eq 7) within the geometry F. The three other diagonal terms E_1^x, E_2^y, and E_2^x, calculated in the same way as E_1^y, lie far above E_1^y (>4000 cm^{-1}). Therefore, the corresponding excited states are not likely to be coupled with the considered S_y state. Under these conditions, the lowest dimer state within geometry F is really a localized S_y state, which confirms the assumption made at the beginning of section 3.3.

The motion of the counterions results not only in a stabilization of S_y but also in a destabilization of the dimer ground state. The total interaction energy calculated for the dimer in the ground state within the geometry F is found to be 2980 cm^{-1} higher than that determined within the geometry G (section 2.3). Consequently, upon relaxation, the energy of the $S_0 \rightarrow S_y$ transition decreases from 18 090 to 13 450 cm^{-1}. The latter value is close to the energy of the fluorescence maximum (13 330 cm^{-1} in fluid nonpolar solvents and 13 890 cm^{-1} in polystyrene films).

After having demonstrated that localization of the excitation is favored by energetic considerations, we examine the relative polarization of the dimer electronic transitions. In Table 5 are listed the angles α_k formed between the dipole moment of the localized $S_0 \rightarrow S_y$ transition and each one of the Franck−Condon transition moments μ^k (Table 3), calculated within the geometry G. They are compared to the corresponding experimental values deduced from the anisotropy associated with each $|0\rangle \rightarrow |k\rangle$ transition (Table 1). To assess the agreement between the calculated and experimental values, we must recall that, for parallel transition moments related to absorption and fluorescence, anisotropy values of 0.3 rather than 0.4 are currently found, indicating a 24° rotation.[34] With this in mind, the agreement of the angles corresponding to the three lower transition is quite good. In particular, the moment of the lowest Franck−Condon transition is found to be quasi orthogonal (α_1 = 78°) to the one corresponding to a localized S_y fluorescent state. The higher difference (32°) observed for the upper in energy transition is attributed to a wrong anisotropy value resulting from the difficulties encountered to fit the spectrum in the blue side.[30] It is also worth noticing that the $S_0 \rightarrow S_y$ transition is an allowed one, in agreement with the short radiative lifetime (<18 ns) determined experimentally.[11]

Finally, we should remark that highly relaxed dimer fluorescence has been observed for xanthene dyes in Langmuir−Blodgett films.[35] The broad and structureless emission band has been considered to be excimer like; relaxation has been interpreted in terms of distance decrease between parallel monomers, resulting in a larger exciton coupling. Our calculations have shown that, in the case of the triarylpyrylium dimers studied here, such a scenario cannot be followed. Indeed, the counterions being sandwiched between the cationic chromophores, the interchromophore distance cannot change significantly. This is corroborated by the fact that the width of the dimer emission band is 2200 cm^{-1} (fwhm), a value usually encountered for monomeric dyes, and a vibrational structure is observed.[10,11]

4. Summary and Conclusions

The present theoretical investigation, based on quantum chemistry methods and the exciton theory, deals with ion-pair dimers formed by 2,6-diphenyl-4-(4′-(dialkylamino)phenyl)-pyrylium tetrafluoroborates. In this companion contribution of a previously published experimental study,[11] it is intended to correlate the properties of the electronic transitions of the triarylpyrylium dimers with the molecular arrangement and the electronic structure of the ionic species (two cations and two anions).

First, the dimer geometry has been determined by minimization of the potential interaction energy calculated at a molecular level using a simulated annealing method. The most stable configuration G corresponds to a noncentrosymmetric oyster-like structure where the two anions are sandwiched between the two pyrylium cores forming an angle of *ca.* 30°. Such a molecular arrangement is in agreement with the fact that no further aggregation is observed in solution and is corroborated by the structural data obtained from ^{1}H-NMR and nonlinear optical measurements.

Next, we have concentrated on the properties of the four Franck−Condon dimer transitions related to two orthogonal and close in energy transitions of the monomer. Taking into account the coupling values deduced from spectral analysis, we have determined the coefficients of the linear combinations describing each dimer excited state. Then, we have shown that the transition moments calculated within the geometry G are close to the transition moments determined experimentally. In particular, we have found that the largest oscillator strength is carried by the third electronic transition.

Finally, we have focused our attention on the relaxation process in the first excited state, leading to a polarization change of *ca.* 90° and a *ca.* 3000 cm^{-1} Stokes shift. Solvent effects cannot account for this relaxation which occurs even in solid matrices. We have demonstrated that the drastic change in the polarization of the lowest transition can be explained by localization of the excitation on one of the two chromophores. Emission from a localized excited state within the considered geometry is in agreement with the fluorescence excitation anisotropy spectra. We have also shown that localization of the excitation is accompanied by a moving of the counterions by *ca.* 1.5 Å, due to the variation of the atomic charge distribution. The calculated decrease (3350 cm^{-1}) in the transition energy upon relaxation is practically the same as the experimentally observed Stokes shift (3000 ± 400 cm^{-1}).

In conclusion, we have correlated the unusual optical properties of the dimers formed by triarylpyrylium salts with an oyster-like geometry and the existence of a charge transfer state for the cationic chromophore. Several fundamental questions arise from this investigation. Is the oyster-like arrangement typical of ion-pair dimers? Do the counterions sandwiched between the chromophores play a role in the exciton coupling? Does the existence of a charge transfer state lead necessarily to

localization of the excitation? What is the dynamics of the relaxation involving counterion motion? In order to elucidate these questions, we started the study of other ionic dyes soluble in nonpolar solvents.

Appendix

The Hamiltonian $\mathbf{H}_0$ of the examined system is represented by the matrix

$$\mathbf{H} = \begin{bmatrix} E_y & 0 & V_{yy} & V_{xy} \\ 0 & E_x & V_{xy} & V_{xx} \\ V_{yy} & V_{xy} & E_y & 0 \\ V_{xy} & V_{xx} & 0 & E_x \end{bmatrix} \tag{14}$$

The four eigenvalues E_k correspond to the excitation energies determined experimentally. In order to find the eigenstates, it is necessary to determine the five components of the matrix. If we assign a certain value to the diagonal term E_x, we can write $\mathbf{H} = E_x\mathbf{I} + \mathbf{H}'$, where $\mathbf{I}$ represents the identity matrix and $\mathbf{H}'$ corresponds to

$$\mathbf{H}' = \begin{bmatrix} \Delta E & 0 & V_{yy} & V_{xy} \\ 0 & 0 & V_{xy} & V_{xx} \\ V_{yy} & V_{xy} & \Delta E & 0 \\ V_{xy} & V_{xx} & 0 & 0 \end{bmatrix} \tag{15}$$

with $\Delta E = E_y - E_x$. The eigenvalues of $\mathbf{H}'$ are given by $\lambda_k = E_k - E_x$, and they are solutions of the secular determinant

$$D = \begin{vmatrix} \Delta E - \lambda & 0 & V_{yy} & V_{xy} \\ 0 & -\lambda & V_{xy} & V_{xx} \\ V_{yy} & V_{xy} & \Delta E - \lambda & 0 \\ V_{xy} & V_{xx} & 0 & -\lambda \end{vmatrix} \tag{16}$$

D corresponds to a fourth−order equation with respect to λ

$$D = \lambda^4 - 2\Delta E\lambda^3 + \{\Delta E^2 - [(V_{yy})^2 + 2(V_{xy})^2 + (V_{xx})^2)]\lambda^2 + 2\Delta E[(V_{xy})^2 + (V_{xx})^2]\lambda + [(V_{xy})^2 - (V_{yy})(V_{xx})]^2 - [(V_{xx})\Delta E)]^2 \tag{17}$$

As λ_k are solutions of D, we have also the expression

$$D = (\lambda - \lambda_1)(\lambda - \lambda_2)(\lambda - \lambda_3)(\lambda - \lambda_4) = \lambda^4 - (\lambda_1 + \lambda_2 + \lambda_3 + \lambda_4)\lambda^3 + [(\lambda_1 + \lambda_2)(\lambda_3 + \lambda_4) + \lambda_1\lambda_2 + \lambda_3\lambda_4]\lambda^2 - [(\lambda_1 + \lambda_2)\lambda_3\lambda_4 + (\lambda_3 + \lambda_4)\lambda_1\lambda_2]\lambda + \lambda_1\lambda_2\lambda_3\lambda_4 \tag{18}$$

By identifying the coefficients of each power of λ, we obtain one system of four equations with four unknowns which are ΔE, V_{yy}, V_{xy}, and V_{xx}

$$\begin{cases} 2\Delta E = \lambda_1 + \lambda_2 + \lambda_3 + \lambda_4 \\ (\Delta E)^2 - [(V_{yy})^2 + 2(V_{xy})^2 + (V_{xx})^2] = (\lambda_1 + \lambda_2)(\lambda_3 + \lambda_4) + \lambda_1\lambda_2 + \lambda_3\lambda_4 \\ 2\Delta E[(V_{xy})^2 + (V_{xx})^2] = -(\lambda_1 + \lambda_2)\lambda_3\lambda_4 - (\lambda_3 + \lambda_4)\lambda_1\lambda_2 \\ [(V_{xy})^2 - (V_{yy})(V_{xx})]^2 - [(V_{xx})\Delta E]^2 = \lambda_1\lambda_2\lambda_3\lambda_4 \end{cases} \tag{19}$$

Resolution of this system provides the values ΔE, V_{yy}, V_{xy}, and V_{xx} for a given E_x value. Then, the Hamiltonian being completely defined, we can determine the coefficients of each eigenstate in the chosen basis by means of the equation

$$H|k\rangle = \lambda_k|k\rangle \tag{20}$$

References and Notes

(1) Graves, R. E.; Rose, P. I. *J. Phys. Chem.* **1975**, *79*, 746.

(2) Hamada, K.; Take, S.; Iijima, T.; Amiya, S. *J. Chem. Soc., Faraday Trans. 1* **1986**, *82*, 3141.

(3) Ishchenko, A. A.; Vasilenko, N. P.; Maidannik, A. G.; Balina, L. V. *Dokl. Akad. Nauk. Ukr. SSR, Ser. B* **1988**, *2*, 46.

(4) Lopez Arbeloa, I.; Ruiz Ojeda, P. *Chem. Phys. Lett.* **1982**, *87*, 556.

(5) Sundström, V.; Gillbro, T. *J. Chem. Phys.* **1985**, *83*, 2733.

(6) Rohatgi-Mukherjee, K. K. *Indian J. Chem.* **1992**, *31A*, 500.

(7) Kasha, M.; Rawls, H. R.; Ashraf El-Bayoumi, M. *Pure Appl. Chem.* **1965**, *11*, 371.

(8) Nüesch, F.; Grätzel, M. *Chem. Phys.* **1995**, *193*, 1.

(9) Markovitsi, D.; Jallabert, C.; Strzelecka, H.; Veber, M. *J. Chem. Soc., Faraday Trans.* **1990**, *86*, 2819.

(10) Lampre, I.; Markovitsi, D.; Birlirakis, N.; Veber, M. *Chem. Phys.* **1996**, *202*, 107.

(11) Lampre, I.; Markovitsi, D.; Fiorini, C.; Charra, F.; Veber, M. *J. Phys. Chem.* **1996**, *100*, 10701.

(12) Markovitsi, D.; Sigal, H.; Ecoffet, C.; Millié, P.; Charra, F.; Fiorini, C.; Nunzi, J. M.; Strzelecka, H.; Veber, M.; Jallabert, C. *Chem. Phys.* **1994**, *182*, 69.

(13) Claverie, P. *Intermolecular Interactions: from Diatomics to Biopolymers*; Pullman, B., Ed.; Wiley: New York, 1978.

(14) Hess, O.; Caffarel, M.; Langlet, J.; Caillet, J.; Huiszoon, C.; Claverie, P. *Proceedings of the 44th International Meeting of Physical Chemistry on Modelling of Molecular Structures and Properties in Physical Chemistry and Biophysics*; Rivail, J. L., Ed.; Elsevier: Amsterdam, 1990.

(15) Brenner, V.; Martrenchard, S.; Millié, P.; Jouvet, C.; Lardeux-Dedonder, C.; Solgadi, D. *Chem. Phys.* **1992**, *162*, 303.

(16) Brenner, V.; Zehnacker, A.; Lahmani, F.; Millié, P. *J. Phys. Chem.* **1993**, *97*, 10570.

(17) Liotard, D. A. *Int. J. Quantum Chem.* **1992**, *44*, 723.

(18) Lampre, I.; Markovitsi, D. Unpublished results.

(19) Flannery, B. P.; Terkolsky, S. A.; Wetterling, W. T. *Numerical Recipes; the Art of Scientific Computing*; Cambridge University Press: Cambridge, 1986.

(20) Momicchioli, F.; Baraldi, I.; Bruni, M. C. *Chem. Phys.* **1983**, *82*, 229.

(21) Marguet, S.; Mialocq, J. C.; Millié, P.; Berthier, G.; Momicchioli, F. *Chem. Phys.* **1992**, *160*, 265.

(22) Allen, F. H.; Kennar, O.; Watson, D. G.; Branner, L.; Orpen, A. G.; Taylor, R. *J. Chem. Soc., Perkin Trans. 2* **1987**, *12*, S1.

(23) Le Fevre, R. J. W. *Advances in Physical Organic Chemistry*; Academic Press: New York, 1965; Vol. III.

(24) Dupuis, M.; Rys, J.; King, W. F. *J. Chem. Phys.* **1976**, *65*, 111 (Program 338, QCPE, Chemistry Department, University of Bloomington, IN).

(25) Ecoffet, C.; Markovitsi, D.; Millié, P.; Jallabert, C.; Strzelecka, H.; Veber, M. *J. Chem. Soc., Faraday Trans.* **1993**, *89*, 457.

(26) Rohatgi, K. K.; Singhal, G. S. *J. Phys. Chem.* **1966**, *70*, 1695.

(27) Mukherjee, P.; Ghosh, A. K. *J. Am. Chem. Soc.* **1970**, *92*, 6419.

(28) Lopez Arbeloa, F.; Llona Gonzalez, I.; Ruiz Ojeda, P.; Lopez Arbeloa, I. *J. Chem. Soc., Faraday Trans. 2* **1982**, *78*, 989.

(29) Ecoffet, C.; Markovitsi, D.; Millié, P.; Lemaistre, J. P. *Chem. Phys.* **1993**, *177*, 629.

(30) The experimental characterization of the dimer electronic transitions was achieved by fitting simultaneously the absorption and excitation anisotropy spectra. The quality of the fit in the blue edge was not as good as in the rest of the anisotropy spectrum (see Figure 3 in ref 11) because of vibrational effects and the appearance of higher transitions.[9] Therefore, the moment and anisotropy values deduced for the $|0\rangle \rightarrow |4\rangle$ transition are less reliable than those of the other three transitions.

(31) Gal, M. E.; Kelly, G. R.; Kurucsev, T. *J. Chem. Soc., Faraday Trans. 2* **1973**, *69*, 395.

(32) Bojarski, C.; Obermueller, G. *Acta Phys. Pol.* **1977**, *A52*, 431.

(33) Markovitsi, D.; Germain, A.; Millié, P.; Lécuyer, P.; Gallos, L.; Argyrakis, P.; Bengs, H.; Ringsdorf, H. *J. Phys. Chem.* **1995**, *99*, 1005.

(34) Valeur, B.; Weber, G. *Photochem. Photobiol.* **1977**, *25*, 441.

(35) Verschuere, B.; Van der Auweraer, M.; De Schryver, F. C. *Chem. Phys.* **1991**, *149*, 385.